

Reaction Kinetics of Concentrated-Acid Hydrolysis for Cellulose and Hemicellulose and Effect of Crystallinity

Pakkapol Kanchanalai,^a Gaurav Temani,^b Yoshiaki Kawajiri,^{a,*} and Matthew J. Realff^a

Batch experiments for the hydrolysis of xylan and pure cellulose (Avicel) hydrolysis and the decomposition of xylose and glucose were performed at varying sulfuric acid concentrations in the range of 10 to 50 wt.% and varying temperatures in the range of 80 to 100 °C. Increasing the temperature and acid concentration hastened the hydrolysis and the sugar decomposition rates. The hydrolysis rate of Avicel was much slower than that of xylan because of its crystallinity. The kinetic parameters for the concentrated acid hydrolysis reaction were estimated for both glucose and xylose reaction paths. The effect of initial cellulose crystallinity on the acid hydrolysis rate was also investigated, such that the cellulose was treated with various concentrations of phosphoric acid. A dramatic reduction in the cellulose crystalline index was observed when the phosphoric acid concentration was in a narrow range around 80 wt.%. It was found that the hydrolysis rate significantly increased with the decrease in initial cellulose crystalline index.

Keywords: Cellulose; Hemicellulose; Concentrated acid hydrolysis; Reaction kinetics; Crystallinity

Contact information: a: School of Chemical & Biomolecular Engineering, Georgia Institute of Technology, 311 Ferst Drive, N.W., Atlanta, GA 30332-0100, USA; b: Department of Chemical Engineering, Birla Institute of Technology & Science, Pilani- K.K Birla Goa Campus, Zuarinagar, Goa 403726, India;

* Corresponding author: ykawajiri@chbe.gatech.edu

INTRODUCTION

An increase in energy demands because of the worldwide population growth and economic expansion as well as uncertainty in fossil fuel prices has created a demand for alternative sources of renewable and sustainable fuel. Lignocellulosic biomass, a second-generation feedstock for bioenergy, is locally available in many countries and has several advantages over non-dispatchable renewable energy sources (EIA 2014). However, the relatively high capital and logistical costs of biomass resources are a significant barrier for its commercial implementation. Considerable effort has been made to develop novel and efficient technologies to convert second generation feedstocks into liquid biofuels (Ho *et al.* 2014).

Biomass contains cellulose, hemicellulose, lignin, and other minor components, and their relative composition varies by source. Cellulose, a polymer of the C6 sugar glucose, is generally the most abundant portion of the biomass and is present primarily in crystalline domains, though a small fraction exists as amorphous material (Kumar *et al.* 2009). Hemicellulose is amorphous, containing both hexoses and pentoses (Dwivedi *et al.* 2009). Although the fermentation process for xylose, the major pentose (C5) in hemicellulose, is not as efficient as that for glucose, the utilization of xylose has been

improved for ethanol production *via* metabolic engineering (Dmytruk *et al.* 2008; Deutschmann and Dekker 2012; Cao *et al.* 2014).

Both hexoses and pentoses can be derived from the hydrolysis of cellulosic biomass, which is usually catalyzed by enzymes or strong acids. Several byproducts from the sugar degradation reaction from acid hydrolysis, especially furfural and hydroxymethylfurfural (HMF), are strong inhibitors of the microbial growth in the fermentation process, necessitating an additional detoxification process (Ranjan *et al.* 2009; Sainio *et al.* 2011; Hanly and Henson 2014). There are other byproducts that are generated from the decomposition of furfural and HMF, including formic and levulinic acid and humins. A possible reaction scheme for biomass hydrolysis is illustrated in Fig. 1.

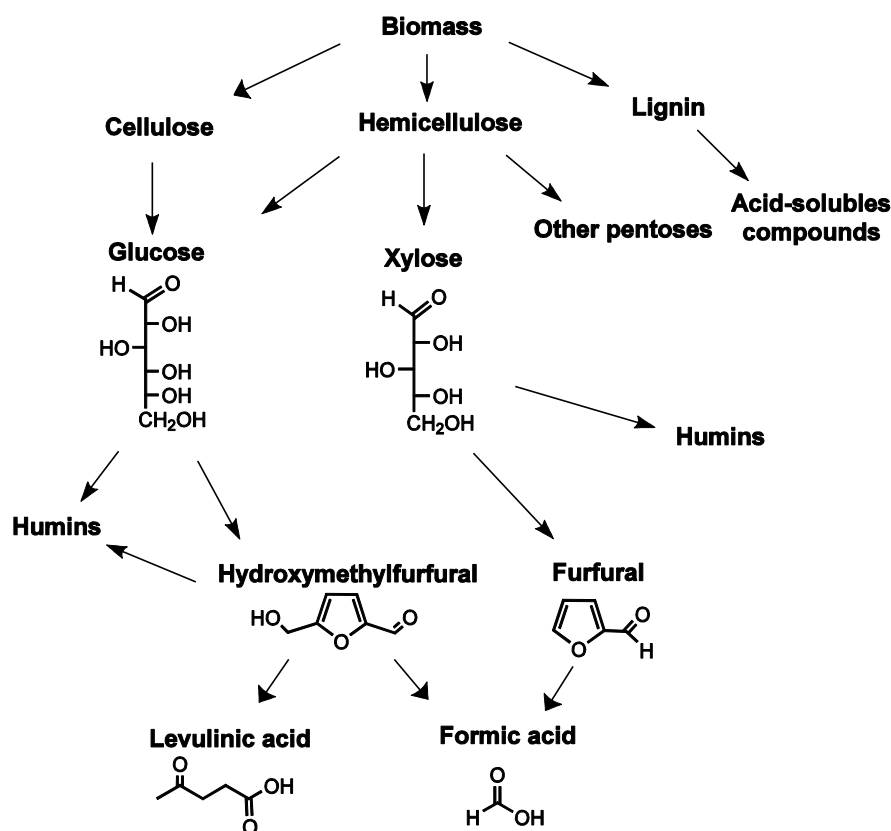


Fig. 1. Possible reaction pathways for biomass acid hydrolysis, Girisuta *et al.* (2006a)

There are several processes that can be used for the first step of converting lignocellulosic biomass into sugars. Concentrated acid hydrolysis has been reported to have several advantages over dilute acid hydrolysis, such as its lower operating temperature and pressure, higher sugar yield, and lower byproduct formation, which are all favorable for the fermentation required for bioethanol production. However, concentrated acid hydrolysis requires specialized materials to prevent corrosion, as well as an acid recovery process, which can significantly increase the cost of saccharification and reduce its economic viability (Tahezadeh and Karimi 2007). Despite these disadvantages, the concentrated acid hydrolysis process has continued to be of interest because of improvements in sugar-acid recovery technologies such as simulated-moving-bed chromatographic separation (Xie *et al.* 2005; Heinonen and Sainio 2012). A concentrated acid hydrolysis process is being developed commercially by Blue Fire Renewable using

chromatographic separation technology that can efficiently recover the sugar without dilution (JGC 2004).

The complex structure of the biomass and its variability in composition make it difficult to predict the kinetics of the hydrolysis reaction. In the enzymatic hydrolysis pathway, for instance, the lignin and hemicellulose content can reduce the accessibility of the catalyst and reduce the rate of hydrolysis (Zhu *et al.* 2008). Furthermore, the variable crystallinity index (CrI) can significantly affect the kinetics of the hydrolysis reaction. Previous work has illustrated a strong correlation between the initial CrI and the initial rate of the enzymatic hydrolysis reaction of the cellulose, such that more amorphous cellulose is hydrolyzed much faster than more crystalline cellulose (Hall *et al.* 2010). In the case of acid hydrolysis, the kinetic parameters of the reactions vary significantly depending on several factors such as the source of the biomass and its different reaction conditions, including temperature and acid concentration (Kanchanalai *et al.* 2014; SriBala and Vinu 2014; Kanchanalai *et al.* 2015). Because of these uncertain factors, modeling the kinetics of the biomass hydrolysis reactions is still a challenge.

The concentrated acid hydrolysis of biomass for sugar production has been addressed only in a few studies (de Paula *et al.* 2012; Janga *et al.* 2012; Lacerda *et al.* 2013). The biomass samples used in these studies contain various compositions of cellulose, hemicellulose, lignin, and various CrI values, which could interfere with the hydrolysis rate of each composition, leading to different reported values for the kinetic parameters. Camacho *et al.* (1996) reported on the kinetic parameters of the concentrated acid hydrolysis of pure cellulose (Merck 2330) and on the glucose decomposition reactions in the low temperature range of 25 to 40 °C and at concentrations of 30% to 70% w/v H₂SO₄ acid. However, this research did not include experimental work on the kinetics of the C5 reaction paths. The concentrated acid hydrolysis process for sugar production is usually performed in two steps, consisting of partial decrystallization at approximately 70 wt.% H₂SO₄ at a low temperature, below 60 °C, and hydrolysis at approximately 20% to 30 wt.% H₂SO₄ at a higher temperature, in the range of 80 to 100 °C (Farone and Cuzens 1997); the kinetics in this temperature range should be investigated more carefully.

The purpose of this paper is to present experimental data and a model of the kinetics of concentrated sulfuric acid cellulose and hemicellulose hydrolysis and of glucose and xylose decomposition reactions. The overarching goal of the research was to obtain the kinetic parameters for a reaction rate model. Pure microcrystalline cellulose (Avicel) and xylan, the major component in hemicellulose, were used in the experiments to separately investigate the kinetics of the C5 and C6 reaction paths. Avicel was used as an ideal simulant for real biomass not containing polysaccharides or lignin, thus avoiding a confounding of the reaction kinetics. The hydrolysate components from the batch experiments, including the sugars and several main decomposed byproducts, were characterized at different temperatures between 80 and 100 °C and at acid concentrations between 10% and 50 wt.% (10% to 70% w/v), which were chosen with the aim of increasing sugar production as well as minimizing byproduct formation. In this study, a relatively simple model was employed so that it could be incorporated into a more extensive process model, such as the solid phase reactive chromatographic separation system (Kanchanalai *et al.* 2014). In addition, the effects of the initial CrI of the cellulose on the rate of the hydrolysis reaction were explored by generating Avicel samples with different crystallinities by exposure to phosphoric acid solutions at various concentrations, a process referred to as decrystallization.

EXPERIMENTAL

Chemicals

Xylan from beechwood (Catalog No. x-4252; Batch No. BCBM5311V), Avicel® PH-101 (Catalog No. 11365; Batch No. BCBJ8498V), which is a microcrystalline cellulose, and xylose, furfural, HMF, levulinic acid, and phosphoric acid (85 wt.%) were purchased from Sigma-Aldrich, (Saint Louis, MO). Formic acid and glucose were purchased from Alfa Aesar (Ward Hill, MA); acetone was purchased from BDH (Muskegon, MI); and sulfuric acid (> 95%) was purchased from MACRON (Center Valley, PA). These chemicals were used for the hydrolysis reaction, cellulose decrystallization, and as standards for high-performance liquid chromatography (HPLC) analysis.

Concentrated Acid Hydrolysis

Batch experiments for the concentrated acid hydrolysis of biomass were carried out to estimate the kinetic parameters of four main reaction paths, including the generation and decomposition of the C5 and C6 sugars. Four sets of batch experiments of the concentrated acid hydrolysis reactions were employed for four different samples, which included xylan, xylose, Avicel, and glucose. Each set of experiments contained six individual batch experiments at various temperatures and H₂SO₄ concentrations, where five of these were used to estimate the optimal experimental parameters and the sixth was used to validate the kinetic model. The treatment of the experimental data sets is discussed in detail in the section discussing parameter estimation. Table 1 summarizes the preparation of samples and the reaction conditions for the batch experiments performed in this work.

Table 1. Batch Experiments for Concentrated Acid Hydrolysis

Batch experiment	Set 1	Set 2	Set 3	Set 4
Reactions	Xylan hydrolysis	Xylose decomposition	Avicel (cellulose) hydrolysis	Glucose decomposition
Initial Concentration (g/L)	40	30	100	30
Batch size				
Reactant (grams)	4.0	3.0	15.0	4.5
H ₂ SO ₄ solution (mL)	100	100	150	150
Batch reaction conditions (H_(acid wt%)-T(°C))				
<i>For parameter estimation</i>				
1	H ₂₀ -T ₈₀	H ₂₀ -T ₁₀₀	H ₂₀ -T ₁₀₀	H ₂₀ -T ₁₀₀
2	H ₄₀ -T ₈₀	H ₃₀ -T ₁₀₀	H ₃₀ -T ₁₀₀	H ₃₀ -T ₁₀₀
3	H ₁₀ -T ₈₀	H ₅₀ -T ₁₀₀	H ₅₀ -T ₁₀₀	H ₅₀ -T ₁₀₀
4	H ₁₀ -T ₉₀	H ₄₀ -T ₈₀	H ₄₀ -T ₈₀	H ₄₀ -T ₈₀
5	H ₁₀ -T ₁₀₀	H ₄₀ -T ₉₀	H ₄₀ -T ₉₀	H ₄₀ -T ₉₀
<i>For model validation</i>				
6	H ₃₀ -T ₈₀	H ₄₀ -T ₁₀₀	H ₄₀ -T ₁₀₀	H ₄₀ -T ₁₀₀

To avoid a temperature drop after mixing, all solid samples and the acid were preheated separately before the reaction was started. The total reaction time for all batch hydrolysis experiments was 7 h. Each mixture was stirred constantly using a mechanical or magnetic stirrer at approximately 360 rpm, and the reactor flasks were constantly heated using a temperature controlled heat bath or heating mantle. All samples were taken at various reaction times and filtered into the HPLC vials using a polyethersulfone (PES) membrane syringe filter, which had a pore size of 0.45 μm, from VWR International

(Radnor, PA) (Catalog No. 28145-505). The HPLC vials were immediately transferred to an ice bath to halt any subsequent reactions before HPLC analysis.

Phosphoric Acid Pretreatment for Cellulose

The effects of the initial CrI of the Avicel on the kinetics of the hydrolysis reaction were also investigated. Phosphoric acid was used to pretreat the Avicel samples to generate different CrIs, which permitted the examination of the effect of CrI on the hydrolysis reaction. The phosphoric acid solvent has been used previously for cellulose decrystallization because of its nontoxic, non-corrosive, and safe properties compared with other inorganic acids (Zhang *et al.* 2009). It has also been shown that the ice-cold phosphoric pretreatment has an insignificant impact on the degree of polymerization (Zhang and Lynd 2005).

The pretreatment procedure using phosphoric acid was modified and scaled up from Hall *et al.* (2010). In this study, 3 mL of deionized water was added to 10 g of Avicel to make a slightly moistened substrate. The Avicel sample was then mixed with 150 mL of ice-cold phosphoric acid (77% to 85 wt.%, 0 °C) and held for 60 min in an ice bath accompanied by constant manual stirring. After the pretreatment, 200 mL of ice-cold acetone (0 °C) was added to the mixture to regenerate the cellulose. The mixture was then vacuum-filtered using a coarse fritted filtered funnel and washed three times with 200 mL of ice-cold acetone (0 °C) and four times with 1 L of deionized water until the pH of the filtrate reached 2.6 to 3.0. The pretreated cellulose was dehydrated by freeze-drying (lyophilization) for two days until the weight of the cellulose changed by less than 0.5 g. The weight of the samples was slightly over the initial dry weight (10 g), which was assumed to be due to residual water. The cellulose was sampled so that a measurement of X-ray diffraction could be conducted, and the remaining portion was utilized for concentrated sulfuric acid hydrolysis. The pretreated Avicel samples of approximately 10 g were preheated to 50 °C and hydrolyzed with 150 mL of 40 wt.% sulfuric acid at 80 °C.

Degree of Cellulose Crystallinity using X-Ray Diffraction

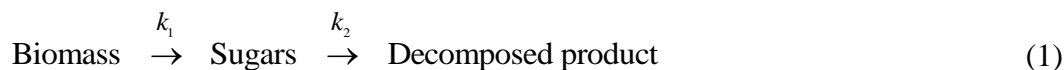
The measurement of CrI of all samples using XRD followed the procedure described by Kang *et al.* (2013). XRD patterns of the lyophilized samples were recorded with an X'pert PRO X-ray diffractometer (PANanalytical BV, Almelo, the Netherlands) using Cu= $K\alpha_1$ irradiation (1.54 Å) at 45 kV and 40 mA. The scattering angle (2θ) ranged from 10° to 40° with a scan speed of 0.021425 s⁻¹ and a step size of 0.0167°.

HPLC Chemical Analyses

The sugar and byproduct components from the hydrolysate samples from the reaction samples were analyzed using HPLC (Shimadzu). A Bio-Rad (Hercules, CA) Aminex HPX-87H column was used, and the analysis was conducted at 50 °C using the eluent of 0.005 M H₂SO₄ at 0.6 mL/min. The injection volumes were 20 µL for all the samples and 3 µL for the samples from the hydrolysis of pretreated Avicel where the calibration curves with corresponding volumes were used to analyze each component. All the samples were stored at 5 °C in the Shimadzu autosampler SIL-20AC during the analysis to stop possible decomposition reactions. The sugars, including glucose and xylose, were detected using a Refractive index RID-10A, while the byproducts, including formic acid, levulinic acid, HMF, and furfural, were detected using a Shimadzu UV-Photodiode Array SPD-M20A at wavelengths of 207, 207, 270, and 310 nm, respectively.

Kinetic Model

Several reaction mechanisms for the hydrolysis of biomass have been considered in previous studies. The reversible transformation between the crystalline and the amorphous structure of the cellulose has been discussed (Mosier *et al.* 2005). The reaction scheme, including the generation of the cellulose nanocrystals, has been addressed in several works (Habibi *et al.* 2010; Kwon *et al.* 2014; Wang *et al.* 2014). Several modifications of the kinetic model, including, for example, the biphasic behavior (Carrasco and Roy 1992; Lu and Mosier 2008; Chen *et al.* 2015), as well as the potential degree of reaction and dissolution (Zhao *et al.* 2014; Dong *et al.* 2015) have also been considered. In the present study, a relatively simple kinetic expression was employed that could be included into the reactive separation system (Kanchanalai *et al.* 2014). Under this consideration, the kinetic model from Saeman (1945) was used to fit the kinetics of the concentrated acid hydrolysis for all reaction paths. Two homogeneous consecutive first-order reactions were assumed in both the cellulose and hemicellulose hydrolysis, as shown in Eq. 1.



The kinetic models for sugar concentration from each set of experiments are shown as follows.

Biomass hydrolysis reaction (experiment set 1 and set 3)

$$\frac{dB_i}{dt} = -k_1 B_i \quad i \in \{\text{xylan, Avicel}\} \quad (2)$$

$$\frac{dC_k}{dt} = k_1 B_i - k_2 C_k \quad (i, k) \in \{(\text{xylan, xylose}), (\text{Avicel, glucose})\} \quad (3)$$

where B and C are the concentrations of biomass and sugar, respectively, and the analytical solution for the sugar concentration is:

$$C_k = \frac{C_{k,eq}^0 k_1}{k_1 - k_2} \left(e^{(-k_2 t)} - e^{(-k_1 t)} \right) \quad k \in \{\text{xylose, glucose}\} \quad (4)$$

where

$$C_{eq}^0 = \frac{\text{initial mass of biomass} \times f_s}{\text{volume of solution}} \times \frac{\text{MW}_{\text{sugar}}}{\text{MW}_{\text{anhydrous sugar}}} \quad (5)$$

Equation 5 shows the expression for the initial equivalent sugar concentration (C_{eq}^0), where f_s is the fraction of sugar consisting in the biomass.

Sugar decomposition reaction (experiment set 2 and set 4)

$$\frac{dC_k}{dt} = -k_2 C_k \quad k \in \{\text{xylose, glucose}\} \quad (6)$$

The analytical solution of the above differential equation is given by:

$$C_k = C_k^0 e^{-k_2 t} \quad k \in \{\text{xylose, glucose}\} \quad (7)$$

The Arrhenius expression was used to estimate the kinetic constant, which depends on the temperature, and the effects of acid concentration were included in the pre-exponential factor (Lee *et al.* 2000) as follows:

$$k_j = k_j^0 C_A^{n_j} e^{-\left(\frac{E_{a_j}}{RT}\right)} \quad j = \{1, 2\} \quad (8)$$

Parameter Estimation

The kinetic parameters of the concentrated acid hydrolysis for both C5 and C6 could be estimated using least-square minimization. Two optimization problems were set up for the reaction paths of C5 and C6, where the objective function was given as follows.

$$\min z = \sum_{j \in S_1} \left(\sum_i (C_{exp,i,j} - C_{cal,i,j})^2 \right) + \sum_{j \in S_2} \left(\sum_i (C_{exp,i,j} - C_{cal,i,j})^2 + \rho (C_j^{in} - C_{prep}^{in})^2 \right) \quad (9)$$

In this objective function, the sum of the squared error of the sugar concentration is minimized where $C_{exp,i}$ is the concentration of sugar at the i^{th} data point of the j^{th} experiment, and C_{cal} is the sugar concentration found from the kinetic model in Eqs. 4 and 7. In this fitting, five batch experiments of the biomass hydrolysis (S_1) and five batch experiments of sugar decomposition (S_2) were used to fit k_1 and k_2 for C5 and C6 sugars (see Eq. 1). The remaining batch experiment from each set was excluded from the minimization and instead used to validate the kinetic parameters (Table 1).

It should be noted that the fraction of xylose consisting in the biomass (f_s in Eq. 4) in xylan was not measured; however, the composition analysis from Kumar *et al.* (2013) for the same product catalog from the same manufacturer showed that this beechwood xylan contained approximately 69.6% xylan. In this fitting, f_s for xylan was estimated from the minimization and compared with this reference. The Avicel contained 100% glucans, and thus $f_s = 1$.

There were six kinetic parameters to be estimated, including the pre-exponent factor (k_0), the exponent of acid concentration (n), and the activation energy (E_a) from Eq. 8 for the two consecutive reactions in Eq. 1 for C5 and C6. The concentration of H_2SO_4 , in % w/v, was used to fit the kinetic parameters (Table 2).

Table 2. Sulfuric Acid Concentration Used to Fit the Kinetic Model

%wt.	10	20	30	40	50
%w/v	10.7	22.8	36.6	52.4	70.0

In addition to the kinetic parameters, the initial concentrations of sugar (C_0) in the five batch experiments of set 2 (C5) and set 4 (C6) were allowed to vary and were estimated from the minimization. This was because the measurement of C_0 was very difficult; the reaction vessel may not have been stirred sufficiently at the beginning of each experiment, and the reaction may have proceeded in the time between sampling and HPLC analysis. Additionally, it was found that these parameters were sensitive to the fitting procedure. Nevertheless, the initial concentration could not be greatly different from the nominal value of $C_{prep}^{in} = 30$ g/L, which was the intended initial concentration for experiments for both C5

and C6. To allow for a somewhat minor deviation from the nominal value, Tikhonov regularization was used in the objective function, Eq. 9, with a small parameter, ρ (Hansen 2010). In this optimization problem, there were 12 degrees of freedom in the C5 fitting and 11 degrees of freedom in the C6 fitting.

RESULTS AND DISCUSSION

The experiments outlined in Table 1 were carried out to investigate the reaction kinetics. In all sets of experiments, the color of the mixture became yellow and then dark brown because the dark insoluble humin particles continued to form as a result of the sugar (xylose and glucose) decomposition reactions. In addition, it was observed that compared to the xylan, the Avicel was much more difficult to solubilize into the liquid mixture because of its more crystalline structure.

Xylan Hydrolysis and Xylose Decomposition

Figure 2 depicts the xylose concentration from xylan hydrolysis over different reaction times from the experiments in set 1. It can be seen that under almost all reaction conditions, the xylose concentration rose rapidly to its maximum and was then reduced because of the sugar decomposition reaction. The effect of temperature can be seen in Fig. 2a, where the concentration of H_2SO_4 was constant at 10 wt.%. In this figure, the xylose concentration can be seen to increase slowly over the course of the seven hours at the reaction temperature of 80 °C. When conducted in the higher temperature range of 90 to 100 °C, the xylose concentration increased more rapidly within the first 60 min, reached its maximum at approximately 28 to 29 g/L, and then remained almost constant with a slight reduction, which indicated a low rate of the xylose decomposition reaction.

The effect of acid concentration can be seen clearly in Fig. 2b, where increasing the concentration of H_2SO_4 under the constant temperature of 80 °C rapidly increased the rate of xylose generation. It can be seen that at 40% H_2SO_4 , the xylose concentration increased quickly to its maximum within the first 15 min, and then it began to decrease more quickly than it had in the other conditions, which indicated a higher xylose decomposition rate.

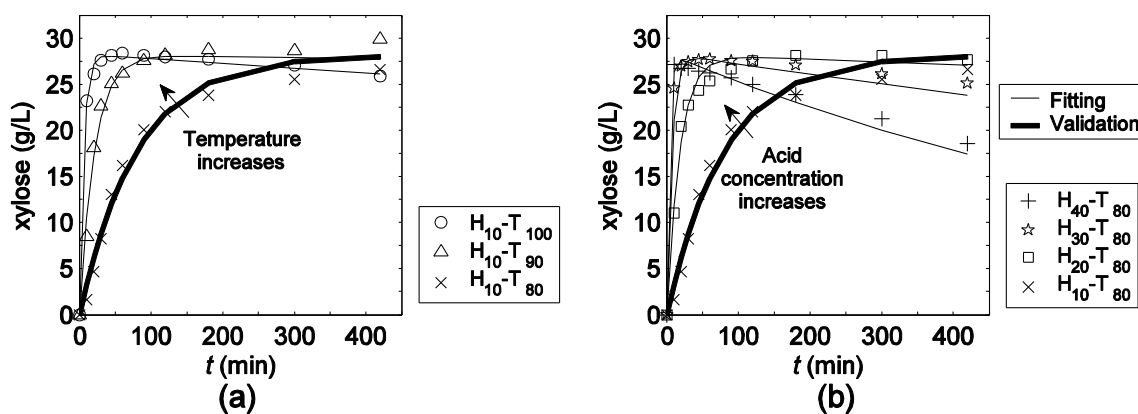


Fig. 2. Xylose concentration from xylan hydrolysis (experiment set 1) as a function of hydrolysis reaction time: (a) 80 to 100 °C at 10 wt.% H_2SO_4 and (b) 10 to 40 wt.% H_2SO_4 at 80 °C

The yield of xylose C / C_{eq}^0 can be calculated from Eq. 4, where f_s could be obtained by solving the optimization problem, which is discussed in the kinetic model fitting section. It was found that a very high xylose yield of more than 95% could be achieved with an appropriate reaction time.

The rate of xylose decomposition was further investigated in the batch experiment set 2, where more severe reaction conditions were employed compared to those used for the xylan hydrolysis (Fig. 3). As can be seen in Fig. 3a, when under constant 10 wt.% H_2SO_4 the temperature was increased, the decomposition rate of xylose also increased, and at 100 °C, the xylose had been completely consumed after approximately 300 min. Likewise, under constant 100 °C, increasing the concentration of H_2SO_4 noticeably increased the decomposition rate of xylose, as shown in Fig. 3b. Under the most severe conditions (50 wt.% H_2SO_4 , 100 °C), the xylose concentration decreased greatly, and then completely decomposed after approximately 90 min.

The xylose decomposition reaction was able to be confirmed from the furfural and formic concentrations, as illustrated in Figs. 4 and 5, respectively. As can be seen in these figures, the concentration of furfural increased rapidly at high temperatures and high concentrations of H_2SO_4 until the concentration reached its maximum, and then was reduced greatly because of the subsequent decomposition to form formic acid. There were also other byproducts, such as humins and some unknown byproducts, which were not quantified.

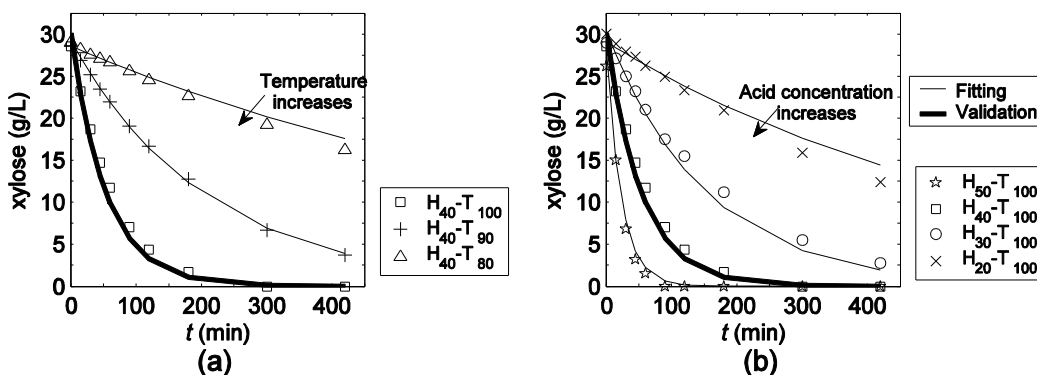


Fig. 3. Xylose concentration from xylose decomposition (experiment set 2) vs. hydrolysis reaction time: (a) 80 to 100 °C at 40 wt.% H_2SO_4 and (b) 20 to 50 wt.% H_2SO_4 at 100 °C

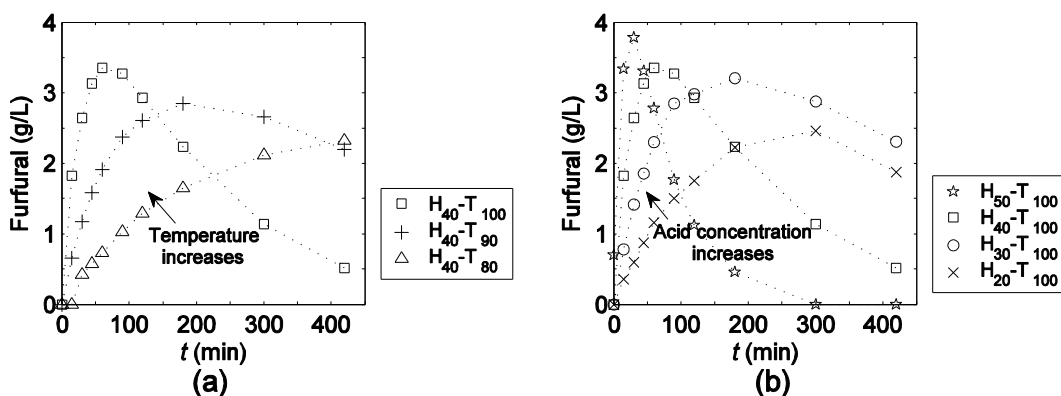


Fig. 4. Furfural concentration from xylose decomposition (experiment set 2) vs. hydrolysis reaction time: (a) 80 to 100 °C at 40 wt.% H_2SO_4 , and (b) 20 to 50 wt.% H_2SO_4 at 100 °C

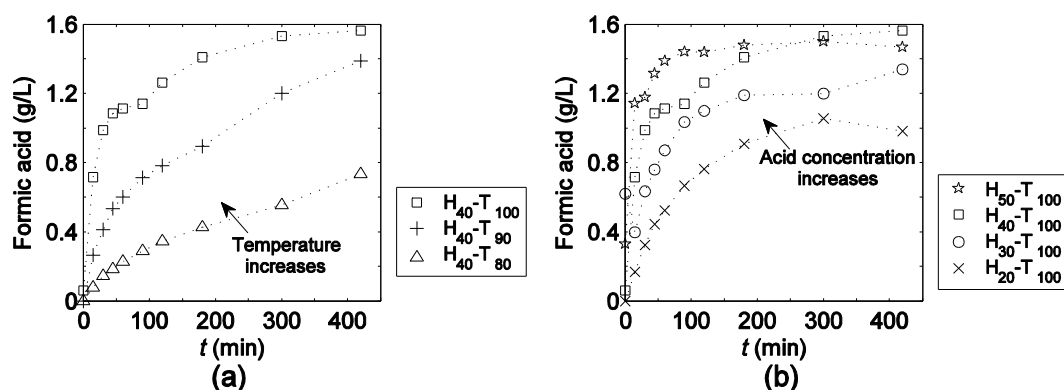


Fig. 5. Formic acid concentration from xylose decomposition (experiment set 2) vs. hydrolysis reaction time: (a) 80 to 100 °C at 40 wt.% H_2SO_4 , and (b) 20 to 50 wt.% H_2SO_4 at 100 °C

Cellulose Hydrolysis and Glucose Decomposition

The concentrations of glucose from the Avicel hydrolysis when subjected to different reaction times (experiment set 3) are illustrated in Fig. 6. As can be seen in the figure, a similar trend could be observed as that between the glucose concentration and the xylose concentration from experiment set 1, such that the concentration of sugar increased with increases in reaction time for most reactions conditions. Figure 6a compares the glucose concentration at different temperature under constant 40 wt.% H_2SO_4 , demonstrating that the glucose concentration increased with temperature.

The effect of changing the H_2SO_4 concentration on the rate of Avicel hydrolysis can be directly seen in Fig. 6b, which depicts a reaction conducted at 100 °C. The glucose concentration increased when the acid concentration was increased from 20 wt.% to 40 wt.%. However, at 50 wt.% H_2SO_4 , the glucose concentration increased with the increase in reaction time and reached its maximum value of 29.0 g/L at approximately 120 min, before decreasing thereafter as a result of the relatively fast glucose decomposition reaction.

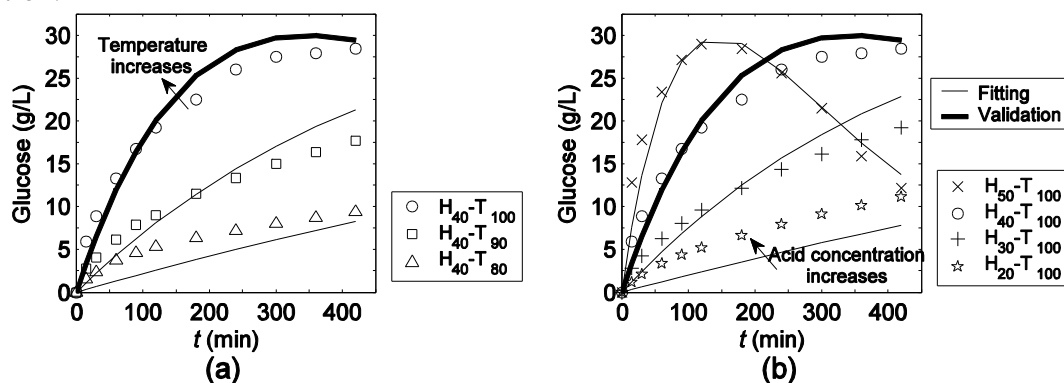


Fig. 6. Glucose concentration from Avicel hydrolysis (experiment set 3) as a function of hydrolysis reaction time: (a) 80 to 100 °C at 40 wt.% H_2SO_4 , and (b) 20 to 50 wt.% H_2SO_4 at 100 °C

It should be noted that the glucose yield (C/C_{eq}^0) under these reaction conditions was approximately 10% to 26%, which is relatively low compared to the xylose yield from the xylan hydrolysis. This relatively low yield indicated a much slower reaction rate for the cellulose hydrolysis reaction because of its crystalline structure.

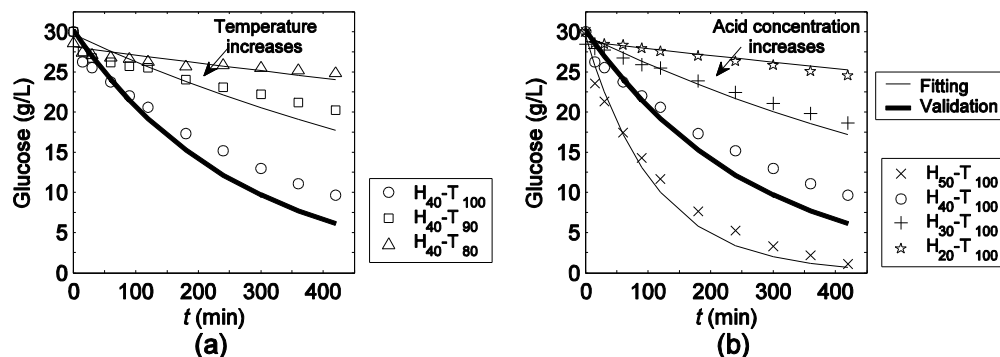


Fig. 7. Glucose concentration from glucose decomposition (experiment set 4) vs. hydrolysis reaction time: (a) 80 to 100 °C at 40 wt.% H_2SO_4 and (b) 20 to 50 wt.% H_2SO_4 at 100 °C

In Fig. 7, the concentration of glucose from the glucose decomposition reaction (experiment set 4) is shown as a function of reaction time. It can be seen that at the constant acid concentration of 40 wt.%, the glucose concentration decreased when the temperature was increased (see Fig. 7a); the decrease in glucose concentration also occurred when the acid concentration was increased (see Fig. 7b) under the constant temperature of 100 °C. By comparing the glucose concentration in Fig. 7 and the xylose concentration in Fig. 3, it can be seen that the glucose decomposed at a much slower rate than the xylose did. The change in the rate of glucose decomposition from this set of experiments was confirmed by an examination of the byproduct concentrations, namely of HMF, formic acid, and levulinic acid, which are illustrated in Figs. 8, 9, and 10, respectively.

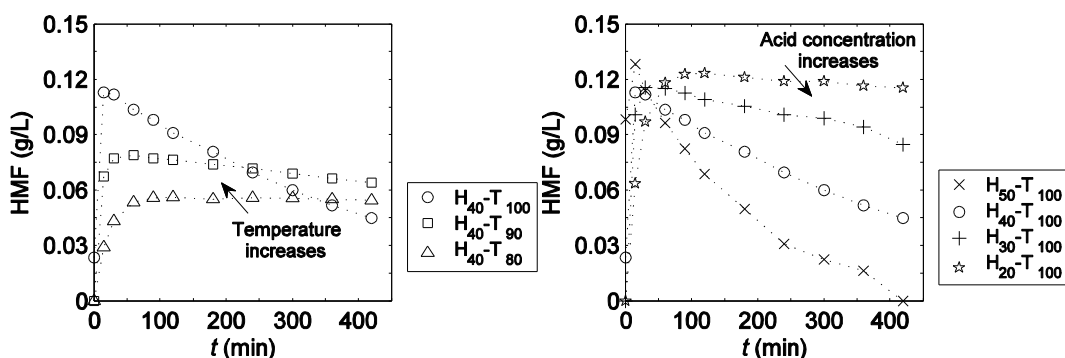


Fig. 8. HMF concentration from glucose decomposition (experiment set 4) vs. hydrolysis reaction time: (a) 80 to 100 °C at 40 wt.% H_2SO_4 and (b) 20 to 50 wt.% H_2SO_4 at 100 °C

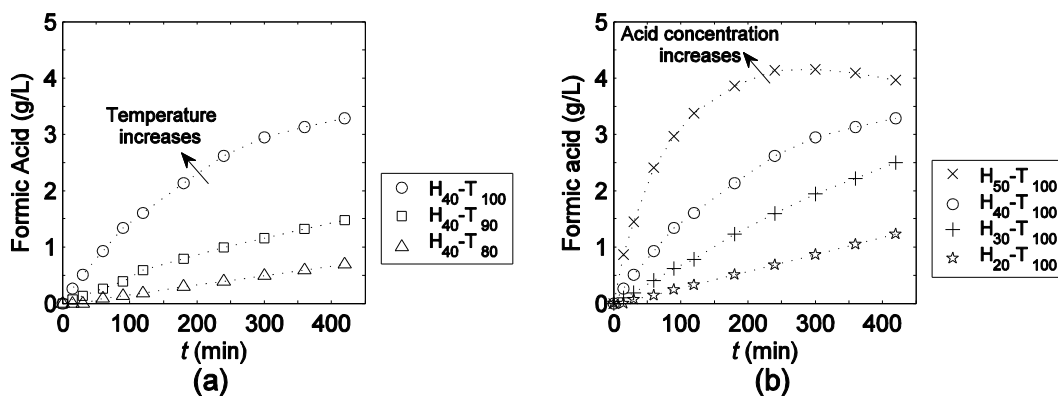


Fig. 9. Formic acid concentration from glucose decomposition (experiment set 4) vs. hydrolysis reaction time: (a) 80 to 100 °C at 40 wt.% H_2SO_4 and (b) 20 to 50 wt.% H_2SO_4 at 100 °C

As can be seen in these figures, the concentration of HMF was relatively low and tended to decrease more quickly at higher temperatures and at higher acid concentrations, which indicated a low stability to the reaction conditions. In contrast, the formic acid and levulinic acid, which are decomposition products of HMF, were the more stable components, as can be seen from their higher concentrations.

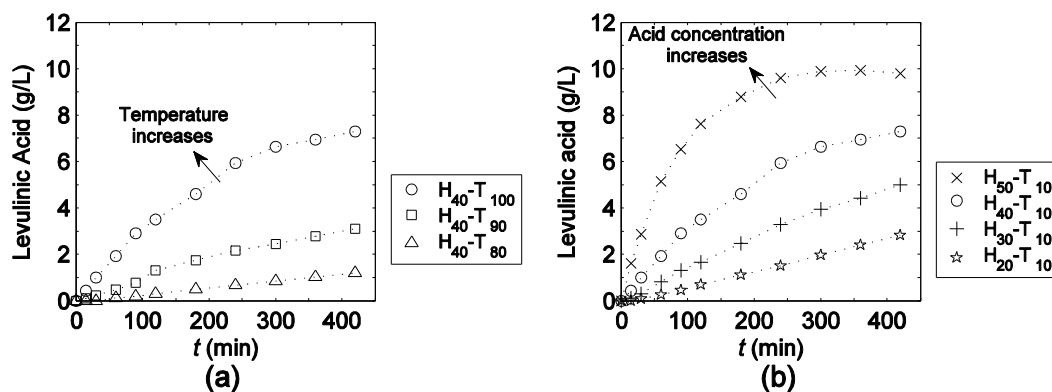


Fig. 10. Levulinic concentration from glucose decomposition (experiment set 4) vs. hydrolysis reaction time: (a) 80 to 100 °C at 40 wt.% H₂SO₄, and (b) 20 to 50 wt.% H₂SO₄ at 100 °C

Some minor inconsistency can be observed regarding the stoichiometry of the byproducts. It has been reported that HMF decomposes into formic and levulinic acid in the molar ratio of 1:1 (Girisuta *et al.* 2006b). However, it was found that the molar concentration of the formic acid was slightly higher than that of the levulinic acid, by up to 30% at the end of the experiment. This could have been due to a potential error in the HPLC analysis whereby some unknown impurities overlapped the peak of formic acid, or a result of unknown reaction paths. Further experiments should be performed to investigate this observation.

Kinetic Model Fitting for Concentrated Acid Hydrolysis

The optimization was carried out using the “fminsearch” function in MATLAB, 2014b, and the optimal values of the kinetic parameters as well as the other estimated parameters found from the minimization are shown in Table 3. As can be seen in the table, the value C^0 of both C5 and C6 only deviated slightly from the nominal value $C_{prep}^{in} = 30$ g/L for all conditions, and the composition of xylan (f_s) was consistent with the analysis from the reference (Kumar *et al.* 2013).

Table 3. Estimated Kinetic Parameters for Each Reaction Path

Parameter	Optimal values		
C_0 (g/L) of xylose in experiment set 2	29.5, 30.2, 29.7, 28.8, 29.6, 28.1		
C_0 (g/L) of glucose in experiment set 4	29.1, 30.5, 30.1, 28.3, 29.3, 28.6		
f_s for xylan	70.6%		
Reactions	k_0 (min ⁻¹ (%w/v) ⁻ⁿ)	n	E_a (kJ/mol)
Xylan hydrolysis	1.42×10^{17}	1.96	142.52
Xylose decomposition	3.15×10^{14}	2.88	151.30
Avicel hydrolysis	2.96×10^{10}	2.94	129.98
Glucose decomposition	1.76×10^{10}	3.00	127.32

In the estimated value of the kinetic parameters shown in Table 3, the activation energy (E_a) of the xylan and xylose was higher than that of Avicel and glucose, which indicated that the rates of the C5 reaction paths were more sensitive to temperature. In terms of the acid concentration, the values of the exponent n for the Avicel hydrolysis and glucose decomposition were similar. However, the value of n for the xylan hydrolysis was lower than that of the xylose decomposition. This means that, compared to the rate of xylan hydrolysis, the rate of xylose decomposition was more sensitive to the acid concentration. Therefore, a very high acid concentration may have not been favorable for the C5 reaction paths because of the higher rate of xylose decomposition.

The fitted model of the C5 paths was compared with the experimental results for each reaction condition (Figs. 2 and 3). Furthermore, the parameters were validated using the estimated values to predict the kinetics of the xylan hydrolysis at H₃₀-T₈₀ in experiment set 1 and kinetics of the xylose decomposition at H₄₀-T₁₀₀ in experiment set 2; a good prediction was observed for both batch experiments. From these results, it could be seen that the mechanism of the first-order kinetic model with two consecutive reactions was sufficiently accurate to estimate the xylose concentration from the concentrated acid hydrolysis of xylan.

Comparisons between the experiment results with the fitted model of C6 for the Avicel hydrolysis and the glucose decomposition reaction are illustrated in Figs. 6 and 7, respectively. As can be seen in Fig. 6b, the predicted glucose yield slightly underestimated the experimental results of the condition H₂₀-T₁₀₀. Therefore, caution should be exercised in using the model at low sulfuric acid concentrations. To further assess the reliability of the model for the C6 path, the model was validated in the prediction of the glucose concentration from the Avicel hydrolysis and glucose decomposition at the reaction condition of H₄₀-T₁₀₀. It can be seen from Fig. 6 that compared with the experimental results, the model gave a satisfactory prediction for the glucose concentration. The prediction of the glucose concentration from glucose decomposition at H₄₀-T₁₀₀ shown in Fig. 7 was slightly lower than that from the experiments. It could be concluded that the first-order two consecutive reaction mechanism shown in Eq. 1 was sufficient to predict the kinetics of the concentrated acid hydrolysis for Avicel and the glucose decomposition reaction.

Some mechanisms were neglected in the models considered in this study. First, the kinetic model used in the work for all reaction paths of C5 and C6 did not consider the effect of mass transfer resistance. A study by Brennan and Wyman (2004) showed that the mass transfer model could explain many features of the biomass hydrolysis for the continuous flowthrough system. Mass transfer is an important phenomenon in the processing of biomass particles, but it is good modeling practice to try to separate the intrinsic kinetics from the mass transfer where possible. In addition, the initial value of CrI of the Avicel was not included in this kinetic model; this is discussed in the next section.

Cellulose Crystallinity Index and Its Effect on Hydrolysis Reaction

Figure 11 shows the CrI of the pretreated Avicel at various phosphoric acid concentrations. It was confirmed that there was a strong correlation between the acid concentration and the CrI, which decreased as acid concentration increased. Whereas the CrI of the non-pretreated Avicel was approximately 56.7%, for the pretreated Avicel, a steep change in CrI was observed in the narrow range of phosphoric acid concentration between 77 and 80 wt.%. On the other hand, a relatively small change was observed when

the acid concentration was greater than 80 wt.%. A very similar trend was also observed in previous work (Hall *et al.* 2010).

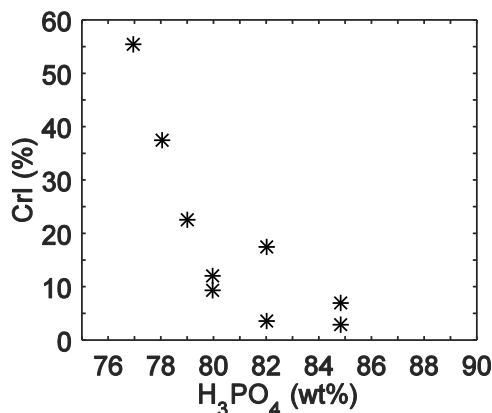


Fig. 11. Effect of phosphoric acid concentration on the crystallinity index

During the pretreatment experiment, a great amount of swelling was observed in the Avicel samples. The swelling was most pronounced at the H₃PO₄ concentration of approximately 80 wt.%, while it was much less pronounced at higher and lower concentrations.

The initial CrI of the Avicel strongly influenced the rate of the hydrolysis reaction. Figure 12a illustrates the glucose yields at different initial CrIs from the 7-h concentrated sulfuric hydrolysis reaction using partially decrystallized Avicel. As can be seen in the figure, for the non-pretreated sample where CrI = 56.7%, the final glucose yield ($t = 420$ min) was approximately 8.4%. The final yield increased to 22% when the initial CrI was nearly 37%, and further increased to 35% when the initial CrI was only 12%. When the initial CrI was smaller than 10%, the samples became almost completely amorphous, which rendered them more accessible and enabled the acid to penetrate and hydrolyze the cellulose, whereupon the final glucose yield increased to approximately 45%. The trend can be seen clearly in Fig. 12b, with a few outliers that may have come from errors in CrI measurement.

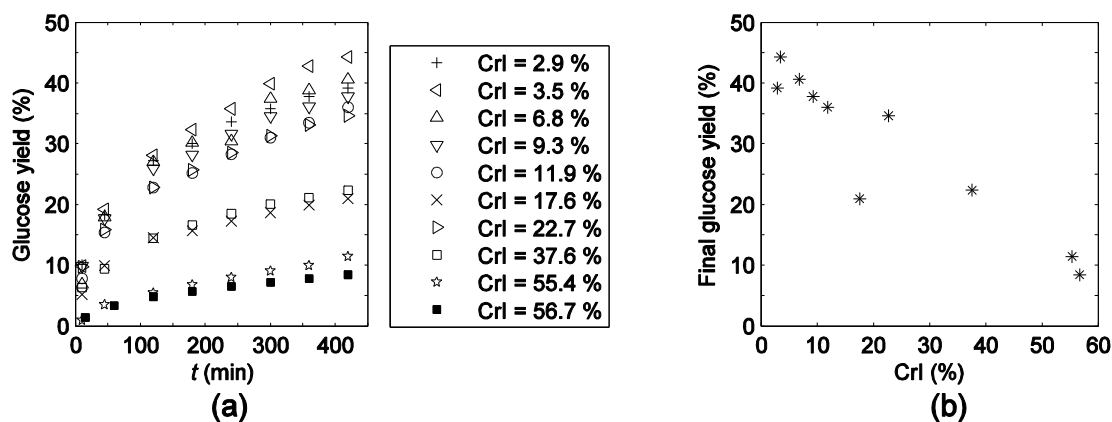


Fig. 12. (a) Glucose yield as a function of hydrolysis reaction time for different initial CrI values and (b) final glucose yield from hydrolysis reaction at different initial CrI values

From these results, it was apparent that the initial CrI had a strong impact on the hydrolysis rate, such that the more amorphous forms of cellulose enabled the acid to penetrate and extract greater amounts of glucose, thereby increasing the glucose yield. Real biomass could have varying values of CrI, and the inclusion of a pretreatment step, which requires an understanding of the kinetics of the hydrolysis reaction of biomass with different initial CrI values, may be necessary to increase the sugar yield. A more complicated kinetic model for cellulose hydrolysis, which includes the effects of CrI, should be further investigated and validated in future work.

CONCLUSIONS

1. Several batch experiments were performed to compare the reaction kinetics of the concentrated acid hydrolysis of microcrystalline cellulose (Avicel) and xylan from beechwood as well as the decomposition of glucose and xylose in the temperature range of 80 to 100 °C and at sulfuric acid concentrations of 10 to 50 wt.%.
2. Using a reaction mechanism that consisted of two consecutive reactions, the kinetic parameters were estimated for the purposes of fitting the model and being able to predict the concentration of sugars; good agreement between the experimental results and the kinetic model was found.
3. Microcrystalline cellulose was pretreated with phosphoric acid at various concentrations to generate samples with different CrI values. It was observed that the initial CrI of the microcrystalline cellulose decrystallized to different extents strongly affected the kinetics of the hydrolysis reaction.

ACKNOWLEDGMENTS

The authors gratefully acknowledge the financial support from PTT Public Company Limited, Thailand.

REFERENCES CITED

- Brennan, M. A., and Wyman, C. E. (2004). "Initial evaluation of simple mass transfer models to describe hemicellulose hydrolysis in corn stover," *Appl. Biochem. Biotech.* 113(1), 965-976. DOI: 10.1385/ABAB:115:1-3:0965
- Camacho, F., Gonzalez-Tello, P., Jurado, E., and Robles, A. (1996). "Microcrystalline-cellulose hydrolysis with concentrated sulphuric acid," *J. Chem. Technol. Biotechnol.* 67(4), 350-356. DOI: 10.1002/(Sici)1097 4660(199612)67:4<350::Aid-Jctb564>3.0.Co;2-9
- Cao, L. M., Tang, X. L., Zhang, X. Y., Zhang, J. T., Tian, X. L., Wang, J. Y., Xiong, M. Y., and Xiao, W. (2014). "Two-stage transcriptional reprogramming in *Saccharomyces cerevisiae* for optimizing ethanol production from xylose," *Metab. Eng.* 24, 150-159. DOI: 10.1016/j.ymben.2014.05.001
- Carrasco, F., and Roy, C. (1992). "Kinetic study of dilute-acid prehydrolysis of xylan-containing biomass," *Wood Sci. Technol.* 26(3), 189-208.

- Chen, L. J., Zhang, H. Y., Li, J. B., Lu, M. S., Guo, X. M., and Han, L. J. (2015). "A novel diffusion-biphasic hydrolysis coupled kinetic model for dilute sulfuric acid pretreatment of corn stover," *Bioresour. Technol.* 177, 8-16. DOI: 10.1016/j.biortech.2014.11.060
- de Paula, M. P., Lacerda, T. M., Zambon, M. D., and Frollini, E. (2012). "Adding value to the Brazilian sisal: Acid hydrolysis of its pulp seeking production of sugars and materials," *Cellulose* 19(3), 975-992. DOI: 10.1007/s10570-012-9674-8
- Deutschmann, R., and Dekker, R. F. H. (2012). "From plant biomass to bio-based chemicals: Latest developments in xylan research," *Biotechnol. Adv.* 30(6), 1627-1640. DOI: 10.1016/j.biotechadv.2012.07.001
- Dmytruk, O. V., Dmytruk, K. V., Voronovsky, A. Y., and Sibirny, A. A. (2008). "Metabolic engineering of the initial stages of xylose catabolism in yeast for the purpose of constructing efficient producers of ethanol from lignocellulosics," *Cytol. Genet.* 42(2), 127-138. DOI: 10.1007/s11956-008-2011-3
- Dong, L., Zhao, X. B., and Liu, D. H. (2015). "Kinetic modeling of atmospheric formic acid pretreatment of wheat straw with "potential degree of reaction" models," *RSC Adv.* 5(27), 20992-21000. DOI: 10.1039/C4ra14634d
- Dwivedi, P., Alavalapati, J. R. R., and Lal, P. (2009). "Cellulosic ethanol production in the United States: Conversion technologies, current production status, economics, and emerging developments," *Energy Sustain. Dev.* 13(3), 174-182. DOI: 10.1016/j.esd.2009.06.003
- EIA (2014). *Annual Energy Outlook 2014 with Projections to 2040*, U.S. Energy Information Administration, Washington, DC.
- Farone, W. A., and Cuzens, J. E. (1997). "Strong acid hydrolysis of cellulosic and hemicellulosic material," U.S. Patent #5,597,714.
- Girisuta, B., Janssen, L. P. B. M., and Heeres, H. J. (2006a). "A kinetic study on the conversion of glucose to levulinic acid," *Chem. Eng. Res. Des.* 84(A5), 339-349. DOI: 10.1205/Cherd05038
- Girisuta, B., Janssen, L. P. B. M., and Heeres, H. J. (2006b). "A kinetic study on the decomposition of 5-hydroxymethylfurfural into levulinic acid," *Green Chem.* 8(8), 701-709. DOI: 10.1039/B518176c
- Habibi, Y., Lucia, L. A., and Rojas, O. J. (2010). "Cellulose nanocrystals: Chemistry, self-assembly, and applications," *Chem. Rev.* 110(6), 3479-3500. DOI: 10.1021/Cr900339w
- Hall, M., Bansal, P., Lee, J. H., Realf, M. J., and Bommaris, A. S. (2010). "Cellulose crystallinity - A key predictor of the enzymatic hydrolysis rate," *FEBS J.* 277(6), 1571-1582. DOI: 10.1111/j.1742-4658.2010.07585.x
- Hanly, T. J., and Henson, M. A. (2014). "Dynamic model-based analysis of furfural and HMF detoxification by pure and mixed batch cultures of *S. cerevisiae* and *S. stipitis*," *Biotechnol. Bioeng.* 111(2), 272-284. DOI: 10.1002/Bit.25101
- Hansen, P. C. (2010). *Discrete Inverse Problems: Insight and Algorithms*, Society for Industrial and Applied Mathematics, Denmark. DOI: 10.1137/1.9780898718836
- Heinonen, J., and Sainio, T. (2012). "Modelling and performance evaluation of chromatographic monosaccharide recovery from concentrated acid lignocellulosic hydrolysates," *J. Chem. Technol. Biotechnol.* 87(12), 1676-1686. DOI: 10.1002/Jctb.3816
- Ho, D. P., Ngo, H. H., and Guo, W. (2014). "A mini review on renewable sources for biofuel," *Bioresour. Technol.* 169, 742-749. DOI: 10.1016/j.biortech.2014.07.022

- Janga, K. K., Oyaas, K., Hertzberg, T., and Moe, S. T. (2012). "Application of a pseudo-kinetic generalized severity model to the concentrated sulfuric acid hydrolysis of pinewood and aspenwood," *BioResources* 7(3), 2728-2741. DOI: 10.15376/biores.7.3.2728-2741
- JGC Corporation. (2004). *NEDO's Application of Arkenol's Concentrated Acid Hydrolysis Technology for the Conversion of Biomass to Ethanol*, (http://bfreinc.com/docs/IZUMI_Status_2004_for_BlueFire_051606.pdf), accessed April 2015.
- Kanchanalai, P., Realff, M. J., and Kawajiri, Y. (2014). "Solid-phase reactive chromatographic separation system: Optimization-based design and its potential application to biomass saccharification via acid hydrolysis," *Ind. Eng. Chem. Res.* 53(41), 15946-15961. DOI: 10.1021/Ie501945j
- Kanchanalai, P., Realff, M. J., and Kawajiri, Y. (2015). "Dynamic modelling and optimal design of the solid-phase reactive chromatographic separation system for biomass saccharification via acid hydrolysis," *Comput. Aided Chem. Eng.* 37, 929-934. DOI: 10.1016/B978-0-444-63578-5.50150-X.
- Kang, Y. Z., Bansal, P., Realff, M. J., and Bommarius, A. S. (2013). "SO₂-catalyzed steam explosion: The effects of different severity on digestibility, accessibility, and crystallinity of lignocellulosic biomass," *Biotechnol Progr.* 29(4), 909-916. DOI: 10.1002/Btpr.1751
- Kumar, P., Barrett, D. M., Delwiche, M. J., and Stroeve, P. (2009). "Methods for pretreatment of lignocellulosic biomass for efficient hydrolysis and biofuel production," *Ind. Eng. Chem. Res.* 48(8), 3713-3729. DOI: 10.1021/Ie801542g
- Kumar, R., Hu, F., Sannigrahi, P., Jung, S., Ragauskas, A. J., and Wyman, C. E. (2013). "Carbohydrate derived-pseudo-lignin can retard cellulose biological conversion," *Biotechnol. Bioeng.* 110(3), 737-753. DOI: 10.1002/Bit.24744
- Kwon, G. J., Kim, D. Y., Oh, C. H., Park, B. H., and Kang, J. H. (2014). "Tailoring the characteristics of carbonized wood charcoal by using different heating rates," *J. Korean Phys. Soc.* 64(10), 1474-1478. DOI: 10.3938/Jkps.64.1474
- Lacerda, T. M., Zambon, M. D., and Frollini, E. (2013). "Effect of acid concentration and pulp properties on hydrolysis reactions of mercerized sisal," *Carbohydr. Polym.* 93(1), 347-356. DOI: 10.1016/j.carbpol.2012.10.039
- Lee, Y. Y., Wu, Z. W., and Torget, R. W. (2000). "Modeling of countercurrent shrinking-bed reactor in dilute-acid total-hydrolysis of lignocellulosic biomass," *Bioresour. Technol.* 71(1), 29-39. DOI: 10.1016/S0960-8524(99)00053-X
- Lu, Y. L., and Mosier, N. S. (2008). "Kinetic modeling analysis of maleic acid-catalyzed hemicellulose hydrolysis in corn stover," *Biotechnol. Bioeng.* 101(6), 1170-1181. DOI: 10.1002/Bit.22008
- Mosier, N., Wyman, C., Dale, B., Elander, R., Lee, Y. Y., Holtzapple, M., and Ladisch, M. (2005). "Features of promising technologies for pretreatment of lignocellulosic biomass," *Bioresour. Technol.* 96(6), 673-686. DOI 10.1016/j.biortech.2004.06.025
- Ranjan, R., Thust, S., Gounaris, C. E., Woo, M., Floudas, C. A., von Keitz, M., Valentas, K. J., Wei, J., and Tsapatsis, M. (2009). "Adsorption of fermentation inhibitors from lignocellulosic biomass hydrolyzates for improved ethanol yield and value-added product recovery," *Micropor. Mesopor. Mater.* 122(1-3), 143-148. DOI: 10.1016/j.micromeso.2009.02.025

- Saeman, J. F. (1945). "Kinetics of wood saccharification - Hydrolysis of cellulose and decomposition of sugars in dilute acid at high temperature," *Ind. Eng. Chem.* 37(1), 43-52. DOI: 10.1021/Ie50421a009
- Sainio, T., Turku, I., and Heinonen, J. (2011). "Adsorptive removal of fermentation inhibitors from concentrated acid hydrolyzates of lignocellulosic biomass," *Bioresour. Technol.* 102(10), 6048-6057. DOI: 10.1016/j.biortech.2011.02.107
- SriBala, G., and Vinu, R. (2014). "Unified kinetic model for cellulose deconstruction via acid hydrolysis," *Ind. Eng. Chem. Res.* 53(21), 8714-8725. DOI: 10.1021/Ie5007905
- Taherzadeh, M. J., and Karimi, K. (2007). "Acid-based hydrolysis processes for ethanol from lignocellulosic materials: A review," *BioResources* 2(3), 472-499. DOI: 10.15376/biores.2.3.472-499
- Wang, Q. Q., Zhao, X. B., and Zhu, J. Y. (2014). "Kinetics of strong acid hydrolysis of a bleached kraft pulp for producing cellulose nanocrystals (CNCs)," *Ind. Eng. Chem. Res.* 53(27), 11007-11014. DOI: 10.1021/Ie501672m
- Xie, Y., Chin, C. Y., Phelps, D. S. C., Lee, C. H., Lee, K. B., Mun, S., and Wang, N. H. L. (2005). "A five-zone simulated moving bed for the isolation of six sugars from biomass hydrolyzate," *Ind. Eng. Chem. Res.* 44(26), 9904-9920. DOI: 10.1021/Ie050403d
- Zhang, Y. H. P., and Lynd, L. R. (2005). "Determination of the number-average degree of polymerization of cellodextrins and cellulose with application to enzymatic hydrolysis," *Biomacromolecules* 6(3), 1510-1515. DOI: 10.1021/Bm049235j
- Zhang, J. H., Zhang, J. Q., Lin, L., Chen, T. M., Zhang, J., Liu, S. J., Li, Z. J., and Ouyang, P. K. (2009). "Dissolution of microcrystalline cellulose in phosphoric acid - Molecular changes and kinetics," *Molecules* 14(12), 5027-5041. DOI: 10.3390/molecules14125027
- Zhao, X. B., Morikawa, Y., Qi, F., Zeng, J., and Liu, D. H. (2014). "A novel kinetic model for polysaccharide dissolution during atmospheric acetic acid pretreatment of sugarcane bagasse," *Bioresour. Technol.* 151, 128-136. DOI: 10.1010/j.biortech.2013.10.036
- Zhu, L., O'Dwyer, J. P., Chang, V. S., Granda, C. B., and Holtzapple, M. T. (2008). "Structural features affecting biomass enzymatic digestibility," *Bioresour. Technol.* 99(9), 3817-3828. DOI: 10.1016/j.biortech.2007.07.033

Article submitted: July 8, 2015; Peer review completed: November 1, 2015; Revised version received and accepted: November 5, 2015; Published: January 4, 2016.
DOI: 10.15376/biores.11.1.1672-1689